Spin wave dispersion based on the quasiparticle self-consistent *GW* method: NiO, MnO and α-MnAs

2008 J. Phys.: Condens. Matter 20 295214

(http://iopscience.iop.org/0953-8984/20/29/295214)

J. Phys.: Condens. Matter **20** (2008) 295214 (9pp) doi:10.1088/0953-8984/20/29/295214

Spin wave dispersion based on the quasiparticle self-consistent GW method: NiO, MnO and α-MnAs

Takao Kotani and Mark van Schilfgaarde

School of Materials, Arizona State University, Tempe, AZ 85287-6006, USA

Received 5 April 2008, in final form 5 June 2008
Published 1 July 2008
Online at stacks.iop.org/JPhysCM/20/295214

Abstract

We present calculations of spin wave dispersions for antiferromagnetic MnO, NiO and ferromagnetic α-MnAs based on the recently developed quasiparticle self-consistent GW method (QSGW); we have already shown that QSGW gave a good quasiparticle picture for MnO and NiO in comparison with optical experiments. To obtain the spin wave dispersions, we have developed a method to calculate the transverse dynamical spin susceptibility in the random-phase approximation. This is a general method applicable not only to QSGW, but also to any first-principle method which gives the non-interacting (one-body) Hamiltonian to represent quasiparticles, e.g. the Kohn–Sham Hamiltonian in the density functional theory. In the method, we first calculate the non-interacting spin susceptibility from the supplied non-interacting Hamiltonian; then we obtain the spin susceptibility where the size of the effective interaction is determined so as to satisfy a sum rule. For MnO and NiO, the obtained spin wave dispersions show good agreement with experiments, in contrast to the cases in the local density approximation (LDA) and in the LDA + U. These results support our claim that the independent-particle picture is powerful enough even for materials like NiO and MnO classified to the Mott insulator, that is, the quasiparticle pictures by QSGW work well to describe their linear responses. For α-MnAs, we find a collinear ferromagnetic ground state in QSGW, while this phase is unstable in the LDA.

(Some figures in this article are in colour only in the electronic version)

1. Introduction

The magnetic linear response is a fundamental property of solids. It is given by the spin susceptibility when the spin–orbit coupling is neglected (as we will do in this paper). The spin susceptibility is equivalent to the spin fluctuations, as can be seen from the fluctuation–dissipation theorem. Low-energy spin fluctuations can control some low-energy phenomena, such as magnetic phase transitions, and contribute to resistivity through spin-flip scattering of electrons. Antiferro(AF)magnetic spin fluctuations can play an important role in high-T_c superconductors [1, 2]. It is also the central quantity entering into the description of quantum-critical phenomena [3, 4]. We expect that reliable first-principle methods to calculate the spin susceptibility should give important clues to understand these phenomena. In this paper, we concentrate on the magnetically ordered systems, where the spin susceptibility should be dominated by spin waves (SW) at low energy.

In spite of the recent development of such methods, we still have a large class of systems where we can hardly calculate the spin susceptibility (or SW), e.g. as discussed in [5]. A typical example is MnO; Solovyev and Terakura gave an analysis for the calculation of its SW energies [6]. Then they showed the main problem is in the non-interacting one-body Hamiltonian H^0 from which we calculate the non-interacting spin susceptibility. The spin wave is calculated from the non-interacting spin susceptibility with a formula in the random-phase approximation where the size of the effective interaction is determined so that the SW energies get to be zero at the wavevector $q \to 0$ limit. H^0 given by the local density approximation (LDA), LDA + U, or even the optimized effective potential [7] are not adequate. In the LDA + U case, they traced the error to a misalignment of the oxygen 2p (O(2p)) bands relative to the Mn(3d) bands. It is impossible to choose the U parameter to correct the misalignment, because the U parameter can only control the exchange splitting within 3d bands. A possibility may be

adding some other parameter in addition to U so as to correct the misalignment; however, such a procedure including more parameters become less universal. This situation is somehow similar to the case of optical response (dielectric function) calculation for semiconductors, where H^0 given by LDA is with too small a bandgap, and thus requires some additional correction like a scissors operator. Our case for the spin susceptibility for MnO is rather worse; LDA supplies too problematic an H^0 to be corrected in a simple manner.

Another possibility is to obtain H^0 by some hybrid functional; it has been shown that it can work as explained below: however, it could be problematic from the view of universality. Muscat, Wander and Harrison claimed that a functional called B3LYP [8, 9] (containing 20% of Fock exchange) works even for solids. However, Franchini *et al* [10] showed that another functional called PBE0 is better than B3LYP in order to obtain better agreement with experiments as for the exchange interaction. PBE0 is a combination of 25% of the Fock exchange with a generalized-gradient approximation (GGA) [11]. However, such functionals could be not so universal, mainly because the effect of screening (and therefore the ratio of the Fock exchange) are dependent on materials. In fact, Moreira *et al* [12] reported that a hybrid functional containing 35% of Fock exchange gives the best results for NiO; the ratio of the Fock exchange is rather different from the case of MnO by Franchini *et al*. This is somehow consistent with the latest careful examinations by Fuchs *et al* [13], and Paier *et al* [14]; these clarify the fact that a hybrid functional should be limited since the screening effects (corresponding to the ratio of the Fock exchange) can be material-dependent. These seem to indicate a difficulty to pick up an universally applicable hybrid functional. This difficulty becomes more problematic when we treat inhomogeneous systems, e.g. to treat the Schottky-barrier problem, where the screening effects are very different on the metal side and on the semiconductor side.

Considering these facts, it is necessary to start from good H^0 without such problems. Our recently developed quasiparticle self-consistent GW method (QSGW) includes the above screened exchange effects in a satisfactory manner [15–22]. QSGW is introduced by Faleev, van Schilfgaarde and Kotani [15] based on the all-electron full potential GW method [23]. QSGW determines a reference system of H^0 representing an optimum quasiparticle (QP) picture in the sense of Landau–Silin Fermi liquid theory. As discussed in [19], QSGW is based on a self-consistent perturbation theory under the assumption that some reasonable QP picture should exist. Thus QSGW is based on the completely different idea from that of the usual full self-consistent GW theory which has serious theoretical problems [19, 24]. QSGW self-consistently determines not only H^0, but also the screened Coulomb interaction W and the Green's function G simultaneously.

Until now, we have shown that QSGW gives QP energies, spin moments, dielectric functions and so on in good agreement with experiments for a wide range of materials. There are systematic but small disagreements with experiments. For example, as shown in figure 1 in [17], we see an error so that calculated bandgaps are systematically larger than those by experiments. A recent development by Shishkin, Marsman and Kresse [21] confirmed our conjecture [17] that the inclusion of the electron–hole correlation effect in W will correct the error. Their method is a simplified version of the full Bethe–Salpeter equation (BSE) for W; it includes only the static and spatially local part of the first-order term in the BSE, based on the procedure given by Sottile, Olevano and Reining [25]. As for MnO and NiO [15, 19], the unoccupied 3d levels relative to the top of the valence band are 1–2 eV too high in comparison with experiments; as for 4f electron systems [16], the unoccupied 4f levels are 3–4 eV too high. Such overestimations will also be well corrected if their method gets to be applicable to these materials. QSGW also shows another type of error, which appears in the localized electrons (typically for core states); e.g. the semicore and occupied d levels for GaAs, ZnS, Cu and so on are a little ($\sim$0.5 eV) too shallow relative to the top of the valence (or to the Fermi energy) [15, 19, 21]. We guess that this error can be due to the following reason. For simplicity, let us consider the self-energy Σ for core states; then the main contribution to the self-energy Σ comes when the hole in the core is running through G in the intermediate process of $\Sigma = \mathrm{i}G \times W$. We guess that the error is mainly because we do not include how W is effectively changed when a hole in the core is running through G (roughly speaking, W should be calculated with adding the hole in the core for such an intermediate process); however, it has not been numerically evaluated yet. Even though we have observed these two types of errors in QSGW, we can say that overall agreements with experiments are rather good in comparison with other available methods. We believe that QSGW is a basis for future development of electronic structure calculations. See [19] and its references.

In this paper, we treat spin susceptibility for MnO and NiO with AF ordering II (AF-II) [26], and α-MnAs based on QSGW. α-MnAs is NiAs-type grown on GaAs epitaxially, thus it is a candidate for spintronics applications [27]. For this purpose, we have newly developed a procedure to calculate the dynamical spin susceptibility at zero temperature. It is a general procedure applicable to any first-principle self-consistent method which determines H^0 to specify the QP, even when H^0 contains non-local potentials as in the Hartree–Fock method. We then apply it to LDA, and to QSGW. After we explain the procedure in section 2, we will show that the SW energies obtained with QSGW are in good agreement with experiments for MnO and NiO. See [19] for dielectric functions for NiO and MnO. For MnAs, our calculation shows that a collinear FM ground state is stable in QSGW though it is not in LDA.

At the end of section 1, we give a discussion to justify using the one-particle picture (band picture) of a 'Mott insulator' for MnO and NiO; it is essentially given by Terakura, Williams, Oguchi and Kübler in 1984 [26] (in the following discussion, 'charge transfer type' or 'Mott type' does not matter). Based on the one-particle picture, the existence of some spin moment (or exchange splitting, equivalently) at each cation site is very essential to make the system insulator. This is consistent with the experimental facts that all the

established 'Mott insulators' are accompanied with the AF (or some) magnetic ordering. Thus the concept 'Mott insulator versus band insulator', often referred to, is misleading, or rather confusing. In order to keep the system insulating, any ordering of spin moment is possible provided the system retains a sufficiently large enough exchange splitting at each site (we need to use the non-collinear mean field method). In this picture, a possible metal–insulator transition at zero temperature (e.g. considering a case to compress NiO) is the first-order transition from a magnetic phase insulator to the non-magnetic metal phase described by a band picture. On the other hand, the transition at finite temperature to a paramagnetic insulator phase occurs because of the entropy effects due to the accumulation of SWs; then the transition is not accompanied by the metal–insulator transition because the exchange splitting (or local moment) at each site is kept even above the Néel temperature T_N. This picture is very different from that assumed in [5, 28], where they emphasize the priority of their method LDA + U+ 'dynamical mean field theory (DMFT)'. In contrast to their claim, we insists that our treatment should be prior and closer to reality for such systems, because of the following reasons.

(i) One-particle treatment in our QSGW allows us to perform parameter-free accurate calculations where we treat all the electrons on the same footing; this is very critical because the relative position of cation 3d bands to O(2p) is important (also their hybridization; we have no SW dispersion without hybridization). Further, we are free from the uncontrollable double-counting problem [29] and do not use a parameter like U which is externally introduced by hand. In contrast, LDA + U + DMFT carries these same problems which are in LDA + U, or rather highly tangled. Thus it is better to take a calculation by LDA + U + DMFT as a model in these cases. As an example, we guess that the distribution probability of the number of 5f electrons in δ-plutonium calculated by LDA + U + DMFT [30] will be easily changed if we shift the relative position (and hybridization) of the 5f band with respect to other bands.

(ii) The DMFT at zero temperature takes into account the quantum-mechanical on-site fluctuation which is not included within the one-particle picture; it allows a system to be an insulator without magnetic order. However, we expect that such quantum-mechanical fluctuation is not essentially important to determine its ground state for materials like NiO and MnO. This is based on our findings that QSGW results can well reproduce the optical response [15, 19], and also the magnetic responses as shown in this paper. These QSGW results are not perfect: however, they supply us with a good enough starting point. For example, in order to describe the d–d multiplet intra transitions (e.g. see figure 6 of [31] by Fujimori and Minami; they are very weak in comparison with interband transitions), it may be easier to start from the cluster models or so; however, parameters used in these models will be determined by QSGW even in such a case.

(iii) At finite temperature, the DMFT can take into account not only such quantum-mechanical fluctuations, but also the on-site thermal fluctuations simultaneously; this is an advantage of DMFT. However, in MnO and NiO, low-energy primary fluctuations are limited to the transverse spin fluctuations except phonons. These can be included in DMFT but it is essentially described by the local-moment disorder [32] as the thermal average of the one-particle picture. Thus there is no advantage of DMFT if only the thermal fluctuations are important.

2. Method for spin susceptibility calculation

In order to calculate the dynamical transverse spin susceptibility, we first perform the self-consistent calculation in LDA and in QSGW. Then we obtain a one-body non-interacting Hamiltonian H^0 which describes the QP in the system. In the following, we will present a method to calculate the susceptibility just from H^0; because of some assumptions and conditions which must be rigorously satisfied (equations (4) and (5)) shown below, we do not need to evaluate the effective interaction explicitly.

We may divide first-principle methods to calculate SW energies into three classes; (A), (B), and (C). (A) is from the Heisenberg Hamiltonian, whose exchange parameters J are determined from the total energy differences of a set of different spin configurations [33–35]. (B) and (C) are based on perturbation. (B) estimates J from static infinitesimal spin rotations [36, 37]. We go through the Heisenberg model even in (B). In contrast, (C) determines SW energies directly from the poles in the transverse spin susceptibility $\chi^{+-}(\mathbf{r}, \mathbf{r}', t-t')$ (defined below) in the random-phase approximation (RPA) or time-dependent LDA (TDLDA) [38–40]. (C) gives the spectrum including lifetime and spin-flip excitations. Because (C) is technically difficult, (A) or (B) have been mainly used. (B) is regarded as a simplification of (C); but real implementations entail further approximations.

Our method belongs to (C). Our formalism is applicable to any H^0 even if it contains non-local potential. At the beginning, we introduce some notations to treat the time-ordered transverse spin susceptibility:

$$\chi^{+-}(\mathbf{r}, \mathbf{r}', t-t') = -\mathrm{i}\langle T(\hat{S}^{+}(\mathbf{r}, t)\hat{S}^{-}(\mathbf{r}', t'))\rangle. \qquad (1)$$

$\langle\cdots\rangle$ denotes the expectation value for the ground state; $T(\cdots)$ means time ordering and $\hat{S}^{\pm}(\mathbf{r}, t) = \hat{S}^{x}(\mathbf{r}, t) \pm \mathrm{i}\hat{S}^{y}(\mathbf{r}, t)$ are the Heisenberg operators of spin density. Since we assume collinear magnetic ordering for the ground state, we have $\langle\hat{S}^{x}(\mathbf{r}, t)\rangle = \langle\hat{S}^{y}(\mathbf{r}, t)\rangle = 0$; $2\langle\hat{S}^{z}(\mathbf{r}, t)\rangle = M(\mathbf{r}) = n^{\uparrow}(\mathbf{r}) - n^{\downarrow}(\mathbf{r})$. $n^{\uparrow}(\mathbf{r})$ and $n^{\downarrow}(\mathbf{r})$ mean up and down electron densities. $M_a(\mathbf{r})$ is the component of $M(\mathbf{r})$ on the magnetic sites a in a unit cell. The Fourier transform of χ^{+-} is

$$\chi^{+-}(\mathbf{T}+\mathbf{r}, \mathbf{r}', \omega) = \frac{1}{N}\sum_{\mathbf{q}} \mathrm{e}^{\mathrm{i}\mathbf{q}\mathbf{T}}\chi^{+-}_{\mathbf{q}}(\mathbf{r}, \mathbf{r}', \omega), \qquad (2)$$

where $\mathbf{T}$ is a lattice translation vector and N is the number of sites. $\mathbf{r}$, $\mathbf{r}'$ are limited to a unit cell.

Next we derive two conditions equations (4) and (5) below, which χ^{+-} rigorously satisfies. Taking the time derivative of

equation (1), we obtain

$$\frac{\partial}{\partial t'}\int \mathrm{d}^3r'\,\chi^{+-}(\mathbf{r}',\mathbf{r},t'-t) = \int \mathrm{d}^3r'\,\langle T([[\hat{H},\hat{S}^+(\mathbf{r}',t')],\hat{S}^-(\mathbf{r},t)])\rangle - \mathrm{i}\int \mathrm{d}^3r'\,\langle[\hat{S}^+(\mathbf{r}',t'),\hat{S}^-(\mathbf{r},t)]\rangle\delta(t'-t), \quad (3)$$

where $[A,B]=AB-BA$. $\hat{H}$ denotes the total Hamiltonian of the system. We have used $\frac{\partial \hat{S}^+(\mathbf{r}',t')}{\partial t'} = \mathrm{i}[\hat{H},\hat{S}^+(\mathbf{r}',t')]$. We assume $\hat{H}$ has rotational symmetry in spin space, so that $[\hat{H},\int \mathrm{d}^3r'\,\hat{S}^+(\mathbf{r}',t')]=0$. Then the first term in the right-hand side is zero. The second term reduces to $M(\mathbf{r})$ because $[\hat{S}^+(\mathbf{r}',t),\hat{S}^-(\mathbf{r},t)] = 2\hat{S}^z(\mathbf{r},t)\delta(\mathbf{r}-\mathbf{r}')$. Thus equation (3) is reduced to be

$$\int_\Omega \mathrm{d}^3r'\,\chi^{+-}_{\mathbf{q}=0}(\mathbf{r}',\mathbf{r},\omega) = \frac{M(\mathbf{r})}{\omega}, \quad (4)$$

where Ω denotes the unit-cell volume. Note that equation (4) is satisfied for any ω. At $\omega\to 0$, this means that $M(\mathbf{r})$ is the eigenfunction of $\chi^{+-}_{\mathbf{q}=0}(\mathbf{r},\mathbf{r}',\omega)$ with divergent eigenvalue; this is because a magnetic ground state is degenerate for homogeneous spin rotation. Another condition is the asymptotic behavior as $\omega\to\infty$. It is given as

$$\chi^{+-}(\mathbf{r}',\mathbf{r},\omega)\to\frac{M(\mathbf{r})}{\omega}\delta(\mathbf{r}-\mathbf{r}')+\mathrm{O}(1/\omega^2). \quad (5)$$

This can be easily derived from the spectrum representation of χ^{+-}. We use equations (4) and (5) to determine the effective interaction $\bar{U}$ in the following.

As in [41], we define the effective interaction $U(\mathbf{r},\mathbf{r}',\omega)$ as the difference between $(\chi^{+-})^{-1}$ and the non-interacting counterpart: $(\chi^{0+-})^{-1}(\mathbf{r},\mathbf{r}',\omega)$:

$$(\chi^{+-})^{-1} = \left(\chi^{0+-}\right)^{-1} + U. \quad (6)$$

In TDLDA, U is the second derivative of the exchange–correlation energy, $U(\mathbf{r},\mathbf{r}') = -\delta^2 E_{\mathrm{xc}}/\delta S^+(\mathbf{r})\delta S^-(\mathbf{r}') = I_{\mathrm{xc}}(\mathbf{r})\delta(\mathbf{r}-\mathbf{r}')$, which is local $U(\mathbf{r},\mathbf{r}')\propto\delta(\mathbf{r}-\mathbf{r}')$, ω-independent and positive. Then we can show that χ^{+-} in TDLDA satisfies condition equations (4) and (5) automatically [42]. In the case of H^0 containing non-local potentials (e.g. in the case of the Hartree–Fock method), U is no longer independent of ω. This is because the natural expansion of χ^{+-} in the many-body perturbation theory requires solving the Bethe–Salpeter equation for the two-body propagator $\chi^{+-}(\mathbf{r}_1,\mathbf{r}_2;\mathbf{r}_3,\mathbf{r}_4,\omega)$. Thus U defined in equation (6) is not directly identified as a kind of diagram. Reference [40] did not pay attention to this point. We can calculate χ^{0+-} in equation (6) as

$$\chi^{0+-}_{\mathbf{q}}(\mathbf{r},\mathbf{r}',\omega) = \sum_{\mathbf{k}n\downarrow}^{\mathrm{occ}}\sum_{\mathbf{k}'n'\uparrow}^{\mathrm{unocc}}\frac{\Psi^*_{\mathbf{k}n\downarrow}(\mathbf{r})\Psi_{\mathbf{k}'n'\uparrow}(\mathbf{r})\Psi^*_{\mathbf{k}'n'\uparrow}(\mathbf{r}')\Psi_{\mathbf{k}n\downarrow}(\mathbf{r}')}{\omega-(\epsilon_{\mathbf{k}'n'\uparrow}-\epsilon_{\mathbf{k}n\downarrow})+\mathrm{i}\delta} + \sum_{\mathbf{k}n\downarrow}^{\mathrm{unocc}}\sum_{\mathbf{k}'n'\uparrow}^{\mathrm{occ}}\frac{\Psi^*_{\mathbf{k}n\downarrow}(\mathbf{r})\Psi_{\mathbf{k}'n'\uparrow}(\mathbf{r})\Psi^*_{\mathbf{k}'n'\uparrow}(\mathbf{r}')\Psi_{\mathbf{k}n\downarrow}(\mathbf{r}')}{-\omega-(\epsilon_{\mathbf{k}n\downarrow}-\epsilon_{\mathbf{k}'n'\uparrow})+\mathrm{i}\delta}, \quad (7)$$

where $\mathbf{k}'=\mathbf{q}+\mathbf{k}$. $\chi^{0+-}(\mathbf{r},\mathbf{r}',\omega=0)$ is a negative definite matrix. Our definition of χ^{+-} and also χ^{0+-} can be different in sign from other definitions in the literature because we start from equation (1).

In order to realize an efficient computational method, we assume that the magnetization is confined to magnetic atomic sites, and we explicitly treat only a degree of freedom of spin rotation per each site. Then we can determine U with the help of equations (4) and (5) as in the following. As a choice to extract the degrees of freedom, we consider a matrix $D(\mathbf{q},\omega)$ as

$$(D(\mathbf{q},\omega))_{aa'} = \int_a \mathrm{d}^3r\int_{a'}\mathrm{d}^3r'\,\bar{e}_a(\mathbf{r})\chi^{+-}_{\mathbf{q}}(\mathbf{r},\mathbf{r}',\omega)\bar{e}_{a'}(\mathbf{r}'), \quad (8)$$

and $D^0(\mathbf{q},\omega)$ defined in the same manner. The dimension of the matrix $D(\mathbf{q},\omega)$ is the number of magnetic sites. Here we define $e_a(\mathbf{r}) = M_a(\mathbf{r})/M_a$ where $M_a=\int_a \mathrm{d}^3r\,M_a(\mathbf{r})$; and define $\bar{e}_a(\mathbf{r})$ so that $\bar{e}_a(\mathbf{r})\propto e_a(\mathbf{r})$ and $\int \mathrm{d}^3r\,\bar{e}_a(\mathbf{r})e_a(\mathbf{r}) = 1$; thus $\bar{e}_a(\mathbf{r}) = e_a(\mathbf{r})/\int_a \mathrm{d}^3r\,(e_a(\mathbf{r}))^2$. Corresponding to equation (6), we define the effective interaction $(\bar{U}(\mathbf{q},\omega))_{aa'}$ as

$$(D(\mathbf{q},\omega))^{-1} = \left(D^0(\mathbf{q},\omega)\right)^{-1} + \bar{U}(\mathbf{q},\omega). \quad (9)$$

For the calculation of $D^0(\mathbf{q},\omega)$ from equation (7), we use the tetrahedron technique [19], which allows us to use fewer $\mathbf{k}$ points in the first Brillouin zone (BZ) than those required for the sampling method [40]. $\bar{U}$ defined in equation (9) should include all the downfolded contributions from all the other degrees of freedom. We now assume that $\bar{U}$ is $\mathbf{q}$-independent and site-diagonal, so that it can be written as $\bar{U}_{aa'}(\mathbf{q},\omega) = U_a(\omega)\delta_{aa'}$. Since equation (4) reduces to a constraint $\sum_{a'}(D(\mathbf{q}=0,\omega))_{a'a} = M_a/\omega$, we determine $\bar{U}_a(\omega)$ from

$$\bar{U}_a(\omega) = \frac{\omega}{M_a}\delta_{aa'} - \left(\frac{\sum_b M_b(D^0(\mathbf{q}=0,\omega))^{-1}_{ba}}{M_a}\right)\delta_{aa'}.$$

With this $\bar{U}_a(\omega)$ for equation (9), we finally have

$$(D(\mathbf{q},\omega))^{-1} = \frac{\omega}{M_a}\delta_{aa'} - \bar{J}(\mathbf{q},\omega), \quad (10)$$

$$\bar{J}(\mathbf{q},\omega) = -\left(D^0(\mathbf{q},\omega)\right)^{-1} + \left(\frac{\sum_b M_b(D^0(\mathbf{q}=0,\omega))^{-1}_{ba}}{M_a}\right)\delta_{aa'}. \quad (11)$$

Equation (5) reduces to $(D(\mathbf{q},\omega))^{-1}_{a'a}\to\frac{\omega}{M_a}\delta_{aa'}$ at $\omega\to\infty$; $(D(\mathbf{q},\omega))^{-1}_{a'a}$ given by equation (10) gives this correct asymptotic behavior. Note that we determine U just from the requirement equation (4) because of our approximations 'on-site only U' and 'a basis per magnetic site'. If we need to go beyond such approximations (e.g. multiple basis per site), it will be necessary to introduce additional information, e.g. a part of $\chi(\mathbf{q},\omega=0)$ evaluated by numerical linear-response calculations (perform the QSGW self-consistent calculations with bias fields). By Fourier transformation, we can transform $(D(\mathbf{q},\omega))_{a'a}$ into $D_{RR'}(\omega)$; the same is also for D^0, J and so on. Here $R=\mathbf{T}a$ is the composite index to specify an atom in the crystal. For later discussion we define

$$J(\mathbf{q},\omega) = -(D^0(\mathbf{q},\omega))^{-1} + \frac{\delta_{aa'}}{D^0_{aa}(\omega)}, \quad (12)$$

where $D^0_{aa}(\omega)$ is shorthand for $D^0_{\mathbf{T}a\mathbf{T}a}(\omega)$; it is **T**-independent. The second term in equation (12) is included just in order to remove the on-site term from J. Then equation (11) can be written as

$$\bar{J}(\mathbf{q},\omega) = J(\mathbf{q},\omega) - \left(\frac{\sum_b M_b J_{ba}(\mathbf{q}=0,\omega)}{M_a}\right)\delta_{aa'}. \quad (13)$$

Here, the second term (on-site term) in equation (12) is irrelevant because of the cancellation between two terms in equation (13).

The preceding development for $(D(\mathbf{q},\omega))^{-1}$ facilitates a comparison with the Heisenberg model, whose Hamiltonian is $\mathcal{H} = -\sum_R \sum_{R'} J^{\mathcal{H}}_{RR'}\,\mathbf{S}_R\cdot\mathbf{S}_{R'}$ ($R = \mathbf{T}a$). As shown in the appendix, the inverse of the susceptibility in the Heisenberg model is

$$(D^{\mathcal{H}}(\mathbf{q},\omega))^{-1} = \frac{\omega}{M_a}\delta_{aa'} - \bar{J}^{\mathcal{H}}(\mathbf{q}), \quad (14)$$

where $M_a = |2\mathbf{S}_R|$. Let us compare equations (14) with (10). This $\bar{J}^{\mathcal{H}}_{aa'}(\mathbf{q})$ is given by equation (A.9), which is almost the same as equation (13); only the difference is whether we use $J^{\mathcal{H}}$ or J. This suggests how to construct the Heisenberg model which reproduces equation (10) as good as possible; a possibility is that we simply assign $J(\mathbf{q},\omega=0)$ (neglecting the ω dependence) as $J^{\mathcal{H}}(\mathbf{q})$. We have confirmed that this approximation is good enough to reproduce SW energies in the case for MnO and NiO. However, it is not true in the case of α-MnAs; then we have used another procedure given by Katsnelson and Lichtenstein [42]: we identify $J(\mathbf{q},\omega =$ (SW energy at $\mathbf{q}$)) as $J^{\mathcal{H}}$. This construction exactly reproduces SW energies calculated from $D^{\mathbf{q},\omega}$.

As a further approximation to calculate $J(\mathbf{q},\omega=0)$, we can expand it in real space as (omit ω for simplicity)

$$-J_{RR'} = (D^0_{RR'})^{-1} - \frac{\delta_{RR'}}{D^0_R} = (D^0_R\delta_{RR'} + D^{0,\mathrm{off}}_{RR'})^{-1} - \frac{\delta_{RR'}}{D^0_R}$$
$$\approx \frac{1}{D^0_R} D^{0,\mathrm{off}}_{RR'} \frac{1}{D^0_{R'}}, \quad (15)$$

where we use equation (12); we use notation that the on-site part $D^0_R = D^0_{RR}$ and the off-site part $D^{0\mathrm{off}}_{RR'} = D^0_{RR'} - D^0_{RR'}\delta_{RR'}$. Here we have used the assumption that $D^{\mathrm{off}}_{RR'}$ are small in comparison with the on-site term D^0_R. This approximation corresponds to the usual second-order perturbation scheme of the total energy; if the spin rotation perfectly follows the rotation of the one-particle potential, $\frac{1}{D^0_R}$ is trivial; it is equal to the difference of the one-particle potential between spins (exchange–correlation potential in the case of the density functional theory) because $\frac{1}{D^0_R}$ is the inverse linear response to determine the one-particle potential for given spin rotation. Essentially the same equation as equation (15) was used in [36, 37]. In some cases, this approximation is somehow mixed up with the 'long wave approximation' to expanding J around $D^0(\mathbf{q}=0)$ [41]; however, they should be differentiated. In order to have a rough estimate of $J_{RR'}$, we can further reduce this to the two-site model as originally presented by Anderson and Hasegawa [43, 44]. For an AF magnetic pair (half-filled case), we obtain the following estimate:

$$J_{RR'} \approx -\frac{1}{D_R} D^{0,\mathrm{off}}_{RR'} \frac{1}{D_{R'}} \sim -\frac{4t^2}{\Delta E_{\mathrm{ex}} M}, \quad (16)$$

Table 1. Magnetic parameters calculated by QSGW and LDA (in parentheses). Muffin-tin radii R for cations were taken to be 2.48 (MnO), 2.33 (NiO), and 2.42 (MnAs) au. M_a is the spin moment within the muffin-tin. Our approximation is equivalent to the assumption for U as $U(\mathbf{r},\mathbf{r}',\omega) = \sum_a (U^0_a + \omega U^1_a + \cdots) e_a(\mathbf{r}) e_a(\mathbf{r}')$ in equation (6). Then U^0_a is written as $U^0_a = \int_a \mathrm{d}^3 r \int_a \mathrm{d}^3 r'\, e_a(\mathbf{r}) e_a(\mathbf{r}') U(\mathbf{r},\mathbf{r}',\omega=0)$. Exchange parameters J_{1+}, J_{1-}, J_2 are shown for MnO and NiO. Total spin moments for MnAs are 7.00 μ_B/cell (QSGW) and 5.89 μ_B/cell (LDA). Our definition of J_{1+}, J_{1-}, J_2 follows that of [6], except we distinguish J_{1+} and J_{1-} [45].

	MnO	NiO	α-MnAs
U^0_a (eV)	2.43 (0.95)	4.91 (1.64)	1.08 (0.93)
M_a (μ_B)	4.61 (4.35)	1.71 (1.21)	3.51 (3.02)
J_{1+} (meV)	−2.8 (−14.7)	−0.77 (0.3)	
J_{1-}	−4.8 (−14.7)	−1.00 (0.3)	
J_2	−4.7 (−20.5)	−14.7 (−28.3)	
T_N or T_c (K)	111	275	510
(Experiment)	122[a]	523[a]	400

[a] Reference [48].

where t denotes the transfer integral and ΔE_{ex} is the on-site exchange splitting. We have used $D_R \sim \frac{M}{\Delta E_{\mathrm{ex}}}$ and $D_{RR'} \sim \frac{M}{\Delta E_{\mathrm{ex}}} \times (\frac{2t}{\Delta E_{\mathrm{ex}}})^2$.

Some additional comments. Our formalism here is not applicable to the non-magnetic systems, where $M(\mathbf{r}) = 0$ everywhere. Then we need to determine U in other ways. A possibility is utilizing the static numerical linear-response calculations; it gives the information of the static ($\omega = 0$) part of $\chi^{+-}_{\mathbf{q}}$ directly (easiest spin-polarization mode at each site). Then it will be possible to determine U from such information together with some additional assumptions. In the case of systems like Gd where the d shell and f shell can polarize separately, we may need to extend our formulation so as to include non-locality of U (e.g. U can be parameterized as U_{ijkl} where i, j, k, l are atomic eigenfunction basis for the d or f channel).

3. Result and discussion

3.1. MnO and NiO

Figure 1 shows the calculated SW energies $\omega(\mathbf{q})$ for MnO and NiO. (We used 1728 k-points in the BZ for all calculations, including MnAs.) $\omega(\mathbf{q})$ calculated from the LDA is too large, as earlier workers have found [5, 6]. The detailed shape of $\omega(\mathbf{q})$ is different from earlier work, however: in [5], peaks in $\omega(\mathbf{q})$ occur near 200 meV for NiO, much lower than what we find. QSGW predicts $\omega(\mathbf{q})$ in good agreement with experimental data.

The difference of results between QSGW and LDA is understood by equation (16). $J_{RR'}$ between nearest AF sites essentially determine the SW energies (exactly speaking, three J parameters as shown in table 1). The LDA severely underestimates ΔE_{ex}. This can be corrected by LDA + U: however, Solovyev and Terakura [6] showed that it fails to reproduce SW energies as we mentioned in the introduction. This means that the transfer t is also wrong in LDA + U; in fact, t is through the hybridization with O(2p)

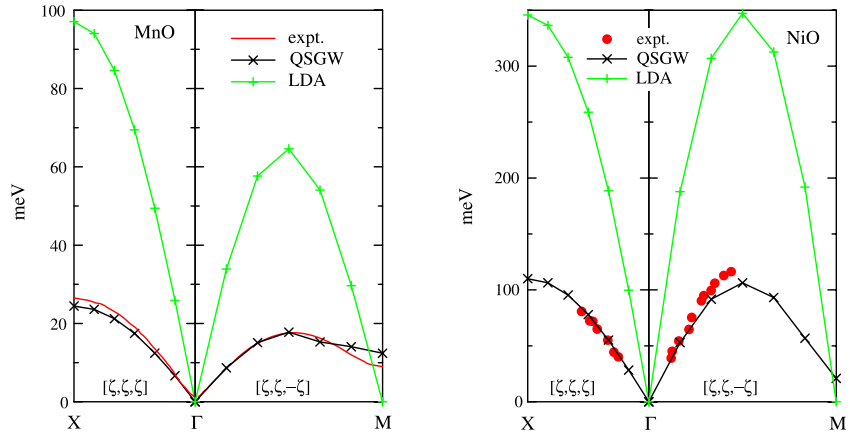

Figure 1. Spin wave dispersion $\omega(\mathbf{q})$ for MnO and NiO calculated from the LDA and QSGW. The solid line without symbols in MnO or dots in NiO (red) are experimental values [45, 46]. We used experimental lattice constants 4.55 and 4.17 Å for MnO and NiO, respectively.

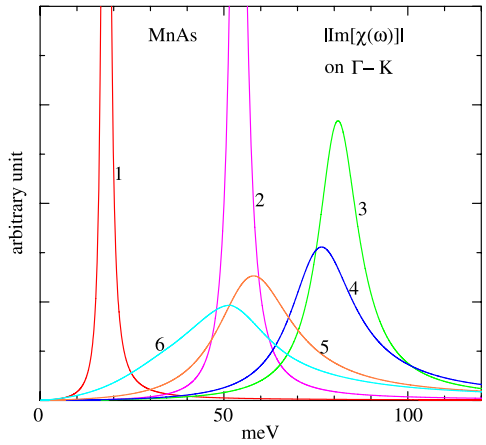

Figure 2. Imaginary part of Tr$[\chi^{+-}(\mathbf{k},\omega)]$ for QSGW. Data are for 6 k-points, all along the $\Gamma-K$ line. The k-point is $i/6$ K (thus $i=6$ falls at K). Peak positions and full width at half-maxima are shown in the $\Gamma-K$ line of figure 3.

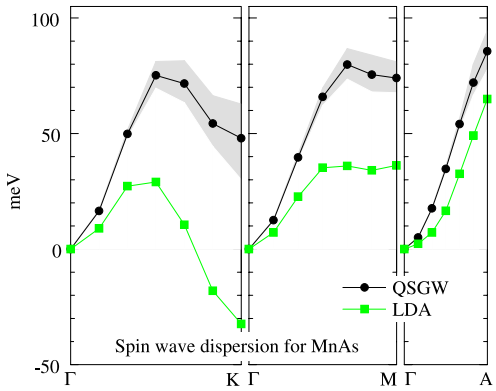

Figure 3. Spin wave dispersion $\omega(\mathbf{q})$ in α-MnAs. QSGW results (circles) are enveloped by hatched regions, which indicate the full width at half-maximum of the spin wave, and is a measure of the rate of SW decay. LDA (squares) predicts negative SW energies around K, indicating that the collinear FM ground state is not stable. The experimental lattice constants $a=3.70$ Å and $c/a=1.54$ were used.

(superexchange). In other words, the agreements with SW experiments in QSGW indicates that both of them are well described by QSGW. Together with the fact that QSGW showed good agreements with optical experiments [15, 19] for MnO and NiO, we claim that our one-particle picture given by QSGW captures the essence of the physics for these systems. Our claim here is opposite to [5, 28] where they claimed that the one-particle picture cannot capture the essence.

3.2. α-MnAs

Because α-MnAs is observed to be an FM with a moment of 3.4 μ_B [47], we construct H^0 assuming an FM ground state. Inspection of the density of states (DOS) in figure 4, shows that QSGW predicts $\Delta E_{ex} \sim$ 1.0 eV larger the LDA. This difference is reflected in the spin moment: $M_a = 3.51\ \mu_B$ in QSGW and 3.02 μ_B in LDA. Figure 2 shows the imaginary part of Tr$[\chi^{+-}(\mathbf{q},\omega)]$ along the $\Gamma-K$ line. Sharp SW peaks are seen at small $\mathbf{q}$; they broaden with increasing $\mathbf{q}$. Figure 3 shows the peak positions, corresponding to SW energies $\omega(\mathbf{q})$. Hatchmarks indicate the full width at half-maximum, extracted from data such as that depicted in figure 2. This corresponds to the inverse lifetime of a SW which decays into spin-flip excitations. (Our calculation gives no width for MnO and NiO, because of the large gap for the spin-flip excitations.) SW peaks are well identified all the way to the BZ boundary. We find that the collinear FM ground state is not stable in the LDA: as figure 3 shows, $\omega(\mathbf{q}) < 0$ around K. (Among all possible *collinear* configurations, the FM state may be the most stable. We did not succeed in finding any collinear configuration more stable than the FM one. A similar conclusion was drawn for the PBE GGA functional [34].) On the other hand, QSGW predicts a stable collinear ground state, that is, $\omega(\mathbf{q}) > 0$ everywhere. However, even in QSGW, the SW energies are still low around K, which is a vector that connects nearest-neighbor Mn sites in the x–y plane. If this SW energy is further lowered for some reason, we may have a frustrated spin system because of the triangle (honeycomb) lattice of the Mn sites. This could be related to the anomalous phase diagram

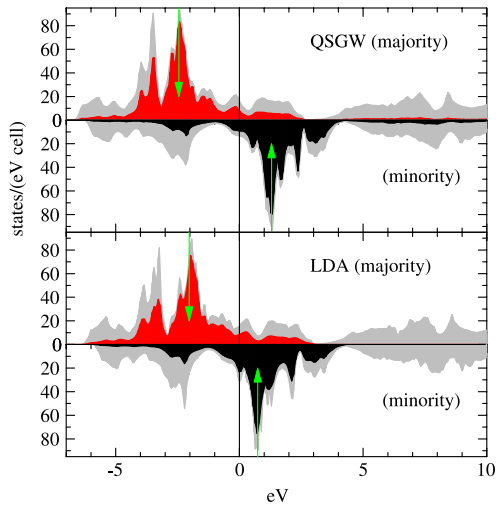

Figure 4. Quasiparticle DOS for α-MnAs. Lighter hatchings indicate total DOS; darker (black and red) hatchings indicate the partial d contribution, whose centers of gravity are shown by arrows. The Fermi energy is at zero.

of MnAs, which can easily occur through the small changes in lattice structure associated with higher-temperature phases.

We can qualitatively understand the difference of SW energies between QSGW and LDA from the difference of $\Delta E_{\rm ex}$. Let us consider the energy difference of FM and AFM states for a two-site model as illustrated in [44]. Then the energy gain of an FM pair is independent of $\Delta E_{\rm ex}$ when some of the majority states are occupied (less than half-filling); we measure the energy from the majority spin's atomic level as the zero. In contrast, the gain of a AFM pair increases with decreasing $\Delta E_{\rm ex}$. Overall, the LDA with its smaller $\Delta E_{\rm ex}$ should contain a stronger AFM tendency.

3.3. Determined parameters and related quantities

Table 1 shows the effective interaction U_a^0 (interaction between unit spins). In NiO and MnO, U_a^0 as calculated by LDA is much smaller than the QSGW result. This is because the LDA underestimates bandgaps in NiO and MnO, thus overestimates the screening. U_a^0 is twice as large in NiO than in MnO. This is because $M_a(\mathbf{r})$ is more localized in NiO; in fact, the QSGW dielectric constants ϵ_∞ are similar ($\epsilon_\infty = 3.8$ (MnO) and 4.3 (NiO) [19]), suggesting that the screened Coulomb interaction $U(\mathbf{r}, \mathbf{r}')$ is similar in the two materials. U_a^0 is smaller in MnAs than in MnO, because it is a metal.

For MnO and NiO, we confirmed that $J_{RR'}$ is non-negligible only for the three nearest neighbors (NN) (table 1). J_{1+} and J_{1-} refer to the first NN, spins parallel and spins antiparallel, respectively. J_2 refers to the second NN [45]. J_{1+} and J_{1-} by QSGW are quite different in MnO, while in LDA $J_{1+} \approx J_{1-}$, resulting in $\omega(\mathrm{M}) \approx 0$ in that case.

For MnAs in QSGW, the expansion coefficients written as $(M^{-1})_{aa'} \equiv \frac{\partial (D^{\mathbf{q}\omega})^{-1}_{aa'}}{\partial \omega}|_{\omega=0}$ is rather dependent on $\mathbf{q}$; nor is $(M^{-1})_{aa'} \propto \delta_{aa'}$. Off-diagonal contributions of $(M^{-1})_{aa'}$ give $\sim$10% contribution to SW energies. In addition, its inverse of the diagonal element $1/(M^{-1})_{aa}$ is reduced by $\sim 0.5\mu_{\rm B}$ at certain points in the BZ. In this case, mapping to a Heisenberg Hamiltonian has a less clear physical meaning.

3.4. Calculation of $T_{\rm N}$ and $T_{\rm c}$ based on the Heisenberg model

From the obtained $J_{RR'}$, we estimated $T_{\rm N}$ ($T_{\rm c}$ for MnAs) for QSGW (table 1) using the cluster variation method adapted to the Heisenberg model [49], which assumes classical dynamics of spins under $\mathcal{H}$. In NiO, the calculated $T_{\rm N}$ is only $\sim$50% of experiment. There are two important effects that explain the discrepancy: (a) QSGW overestimates the d–d exchange splitting [17, 19] and (b) is the classical treatment of quantum dynamics of spins under $\mathcal{H}$. Both effects will increase $T_{\rm N}$. Considering that QSGW well reproduces SW energies (figure 1), the errors connected with (a) would not seem to be so serious in MnO and NiO. (b) can be rather important, especially when the local moment is small. This is a general problem as discussed in [5]: Heisenberg parameters that reproduce SW energies well in NiO do not yield a correspondingly good $T_{\rm N}$. If we multiply our classical $T_{\rm N}$ by a factor $S(S+1)/S^2 \approx 1.86$ (as $2S = M_a = 1.71$), which is the ratio of quantum to classical $T_{\rm N}$ in mean field theory, we have better agreement with experiment. This is what Hutching *et al* used [46]. On the other hand, evaluation of the quantum Heisenberg model using a Green's function technique shows that the mean field theory rather strongly overestimates quantum corrections [50]. Also, $T_{\rm N}$ is already close to the experimental value in MnO. This is explained in part because the correction (b) is less important in MnO, since S is larger. Further, we have large contributions to $T_{\rm N}$ from $J_{1\pm}$ in MnO, but not in NiO. Around $T_{\rm N}$, J_{1+} and J_{1-} will tend to approach some average value, which reduces $\omega(\mathbf{q})$ and therefore $T_{\rm N}$ (recall $\omega(\mathrm{M}) = 0$ when $J_{1+} = J_{1-}$). The temperature dependence of J is not accounted for here.

$J_{RR'}$ exhibits long-ranged, oscillatory behavior in MnAs: its envelope falls off as $|\mathbf{R}-\mathbf{R}'|^3$ as predicted by RKKY theory for a metal. Consequently, it is not so meaningful to estimate $T_{\rm c}$ from just a few NN, as was done recently [34, 35]. Shells up to 25th nearest neighbors are required to converge $T_{\rm c}$ to within 5% or so. The calculated $T_{\rm c}$ is 110K too high in comparison with experiment. Taking (a) into account will improve the agreement; however, there are many factors that make a precise calculation very difficult. We also need to take (b) into account; in addition, other factors, such as assumptions within the Heisenberg model, may give non-negligible contributions.

In conclusion, we present a simple method to calculate spin susceptibility, and applied it in the QSGW method. SW energies for MnO and NiO are in good agreement with experiments; in α-MnAs the FM ground state is stable, which also agrees with experiment (to our knowledge, no SW energies have been published for α-MnAs). LDA results come out very differently in each material. By mapping to the Heisenberg model, we estimated $T_{\rm N}$ or $T_{\rm c}$. We found some disagreement with experiments and discussed some possible explanations.

Acknowledgments

We thank M I Katsnelson, W R Lambrecht, and V P Antropov for valuable discussions. This work was supported by DOE

contract DE-FG02-06ER46302. We are also indebted to the Ira A. Fulton High Performance Computing Initiative.

Appendix. Static $J(q)$ calculation—Heisenberg model

We derive the linear response to an external magnetic field $\mathbf{B}$ for the Heisenberg model, whose Hamiltonian is given as

$$\mathcal{H} = -\sum_{\mathbf{T}a}\sum_{\mathbf{T}'a'} J_{\mathbf{T}a\mathbf{T}'a'}\mathbf{S}_{\mathbf{T}a}\cdot\mathbf{S}_{\mathbf{T}'a'} + g\mu_{\mathrm{B}}\sum_{\mathbf{T}a}\mathbf{S}_{\mathbf{T}a}\cdot\mathbf{B}_{\mathbf{T}a}, \quad \text{(A.1)}$$

where $\mathbf{S}_{\mathbf{T}a}$ is the spin at $\mathbf{T}a$ ($\mathbf{T}$ is for primitive cell, a specify the magnetic site in a cell). $J_{\mathbf{T}a\mathbf{T}a} = 0$. $J_{\mathbf{T}a\mathbf{T}'a'} = J_{\mathbf{T}'a'\mathbf{T}a}$. The equation of motion $-\mathrm{i}\hbar\dot{\mathbf{S}}_{\mathbf{T}a} = [\mathcal{H}, \mathbf{S}_{\mathbf{T}a}]$ is written as

$$\hbar\dot{\mathbf{S}}_{\mathbf{T}a} = \mathbf{S}_{\mathbf{T}a}\times\left(2\sum_{\mathbf{T}'a'} J_{\mathbf{T}a\mathbf{T}'a'}\mathbf{S}_{\mathbf{T}'a'} - g\mu_{\mathrm{B}}\mathbf{B}_{\mathbf{T}a}\right). \quad \text{(A.2)}$$

We introduce $g\mu_{\mathrm{B}}\mathbf{B} = 2\mathbf{b}$ and $\mathbf{S}_{\mathbf{T}a} = \mathbf{S}^0_{\mathbf{T}a} + \Delta\mathbf{S}_{\mathbf{T}a}$. $\mathbf{S}^0_{\mathbf{T}a}$ is the static spin configuration. Then equation (A.2) reduces to

$$\begin{aligned}\hbar\Delta\dot{\mathbf{S}}_{\mathbf{T}a} &= \mathbf{S}^0_{\mathbf{T}a}\times\left(2\sum_{\mathbf{T}'a'} J_{\mathbf{T}a\mathbf{T}'a'}\Delta\mathbf{S}_{\mathbf{T}'a'}\right) + \Delta\mathbf{S}_{\mathbf{T}a}\\ &\quad\times\left(2\sum_{\mathbf{T}'a'} J_{\mathbf{T}a\mathbf{T}'a'}\mathbf{S}_{\mathbf{T}'a'}\right) - 2\mathbf{S}^0_{\mathbf{T}a}\times\mathbf{b}_{\mathbf{T}a}\\ &= \sum_{\mathbf{T}'a'}\left(2\mathbf{S}^0_{\mathbf{T}a}J_{\mathbf{T}a\mathbf{T}'a'}\right)\times\Delta\mathbf{S}_{\mathbf{T}'a'} - \left(2\sum_{\mathbf{T}'a'} J_{\mathbf{T}a\mathbf{T}'a'}\mathbf{S}^0_{\mathbf{T}'a'}\right)\\ &\quad\times\Delta\mathbf{S}_{\mathbf{T}a} - 2\mathbf{S}^0_{\mathbf{T}a}\times\mathbf{b}_{\mathbf{T}a}. \end{aligned} \quad \text{(A.3)}$$

Introducing the Fourier transform, $\Delta\mathbf{S}_{\mathbf{T}a} = \frac{1}{N}\sum_{\mathbf{k}}\Delta\mathbf{S}_a(\mathbf{k})\,\mathrm{e}^{\mathrm{i}\mathbf{k}(\mathbf{T}+\mathbf{a})}$, equation (A.3) reduces to

$$\begin{aligned}\hbar\Delta\dot{\mathbf{S}}_a(\mathbf{k}) &= \sum_{a'}\left(2\mathbf{S}^0_a J_{aa'}(\mathbf{k}) - \left(2\sum_{a''} J_{aa''}(0)\mathbf{S}^0_{a''}\right)\delta_{aa'}\right)\\ &\quad\times\Delta\mathbf{S}_{a'}(\mathbf{k}) - 2\mathbf{S}^0_a\times\mathbf{b}_a(\mathbf{k}). \end{aligned} \quad \text{(A.4)}$$

Assuming $\Delta\mathbf{S}_a(\mathbf{k}) \propto \mathrm{e}^{-\mathrm{i}\omega t/\hbar}$, we have

$$\begin{aligned}&\sum_{a'}\left(\frac{\mathrm{i}\omega\delta_{aa'}}{2} + \mathbf{S}^0_a J_{aa'}(\mathbf{k}) - \left(\sum_{a''} J_{aa''}(0)\mathbf{S}^0_{a''}\right)\delta_{aa'}\right)\\ &\quad\times\Delta\mathbf{S}_{a'}(\mathbf{k}) = \mathbf{S}^0_a\times\mathbf{b}_a(\mathbf{k}). \end{aligned} \quad \text{(A.5)}$$

Let us consider the collinear ground state. Then $\mathbf{S}^0_a = S_a\mathbf{e}_z$ (S_a is the size of spin, including sign). We have

$$\begin{aligned}&\sum_{a'}\left(\frac{\mathrm{i}\omega\delta_{aa'}}{2S_a}\right)\Delta\mathbf{S}_{a'}(\mathbf{k})\\ &\quad+\sum_{a'}\left(J_{aa'}(\mathbf{k}) - \left(\sum_{a''}\frac{1}{S_a}J_{aa''}(0)S_{a''}\right)\delta_{aa'}\right)\mathbf{e}_z\\ &\quad\times\Delta\mathbf{S}_{a'}(\mathbf{k}) = \mathbf{e}_z\times\mathbf{b}_a(\mathbf{k}). \end{aligned} \quad \text{(A.6)}$$

Using $\mathbf{S} = S^+\frac{\mathbf{e}_x-\mathrm{i}\mathbf{e}_y}{2} + S^-\frac{\mathbf{e}_x+\mathrm{i}\mathbf{e}_y}{2} + S^z\mathbf{e}_z$, and $\mathbf{e}_z\times(\mathbf{e}_x\pm\mathrm{i}\mathbf{e}_y) = \mp\mathrm{i}(\mathbf{e}_x\pm\mathrm{i}\mathbf{e}_y)$ we have

$$\sum_{a'}\left(\frac{\omega\delta_{aa'}}{2S_a} - \bar{J}_{aa'}(\mathbf{k})\right)S^+_{a'}(\mathbf{k}) = b^+_a(\mathbf{k}). \quad \text{(A.7)}$$

$$\sum_{a'}\left(\frac{\omega\delta_{aa'}}{2S_a} + \bar{J}_{aa'}(\mathbf{k})\right)S^-_{a'}(\mathbf{k}) = b^-_a(\mathbf{k}), \quad \text{(A.8)}$$

where

$$\bar{J}_{aa'}(\mathbf{k}) = J_{aa'}(\mathbf{k}) - \left(\sum_{a''}\frac{1}{S_a}J_{aa''}(0)S_{a''}\right)\delta_{aa'}. \quad \text{(A.9)}$$

Only the difference between $\bar{J}_{aa'}(\mathbf{k})$ and $J_{aa'}(\mathbf{k})$ are diagonal parts. These are determined so that $\int \mathrm{d}^3k\, J_{aa}(\mathbf{k}) = 0$. Equation (A.7) is the same as equation (14).

References

[1] Moriya T, Takahashi Y and Ueda K 1990 *J. Phys. Soc. Japan* **59** 2905
[2] Millis A J, Monien H and Pines D 1990 *Phys. Rev.* B **42** 167
[3] Lonzarich G G and Taillefer L 1985 *J. Phys. C: Solid State Phys.* **18** 4339
[4] Kaul S N 1999 *J. Phys.: Condens. Matter* **11** 7597
[5] Wan X, Yin Q and Savrasov S Y 2006 *Phys. Rev. Lett.* **97** 266403
[6] Solovyev I V and Terakura K 1998 *Phys. Rev.* B **58** 15496
[7] Kotani T 1998 *J. Phys.: Condens. Matter* **10** 9241
[8] Muscat J, Wander A and Harrison N M 2001 *Chem. Phys. Lett.* **342** 397 33
[9] Becke A D 1993 *J. Chem. Phys.* **98** 5648
[10] Franchini C, Bayer V, Podloucky R, Paier J and Kresse G 2005 *Phys. Rev.* B **72** 045132
[11] Perdew J P, Burke K and Ernzerhof M 1996 *Phys. Rev. Lett.* **77** 3865
[12] de Moreira P R I, Illas F and Martin R L 2002 *Phys. Rev.* B **65** 155102
[13] Fuchs F, Furthmuller J, Bechstedt F, Shishkin M and Kresse G 2007 *Phys. Rev.* B **76** 115109
[14] Paier J, Marsman M and Kresse G 2007 *J. Chem. Phys.* **127** 024103
[15] Faleev S V, van Schilfgaarde M and Kotani T 2004 *Phys. Rev. Lett.* **93** 126406
[16] Chantis A N, van Schilfgaarde M and Kotani T 2006 *Phys. Rev. Lett.* **96** 086405
[17] van Schilfgaarde M, Kotani T and Faleev S 2006 *Phys. Rev. Lett.* **96** 226402
[18] Chantis A N, van Schilfgaarde M and Kotani T 2007 *Phys. Rev.* B **76** 165126
[19] Kotani T, van Schilfgaarde M and Faleev S V 2007 *Phys. Rev.* B **76** 165106
[20] Bruneval F, Vast N, Reining L, Izquierdo M, Sirotti F and Barrett N 2006 *Phys. Rev. Lett.* **97** 267601
[21] Shishkin M, Marsman M and Kresse G 2007 *Phys. Rev. Lett.* **99** 246403
[22] Lukashev P, Lambrecht W R L, Kotani T and van Schilfgaarde M 2007 *Phys. Rev.* B **76** 195202
[23] Kotani T and van Schilfgaarde M 2002 *Solid State Commun.* **121** 461
[24] Holm B and von Barth U 1998 *Phys. Rev.* B **57** 2108
[25] Sottile F, Olevano V and Reining L 2003 *Phys. Rev. Lett.* **91** 056402
[26] Terakura K, Williams A R, Oguchi T and Kübler J 1984 *Phys. Rev. Lett.* **52** 1830
[27] Tanaka M *et al* 1994 *J. Vac. Sci. Technol.* B **12** 1091
[28] Kunes J, Anisimov V I, Skornyakov S L, Lukoyanov A V and Vollhardt D 2007 *Phys. Rev. Lett.* **99** 156404
[29] Petukhov A G, Mazin I I, Chioncel L and Liechtenstein A I 2003 *Phys. Rev.* B **67** 153106
[30] Shim J H, Haule K and Kotliar G 2007 *Nature* **446** 513–6

[31] Fujimori A and Minami F 1984 *Phys. Rev.* B **30** 957
[32] Akai H and Dederichs P H 1993 *Phys. Rev.* B **47** 8739
[33] Connolly J W D and Williams A R 1983 *Phys. Rev.* B **27** 5169
[34] Rungger I and Sanvito S 2006 *Phys. Rev.* B **74** 024429
[35] Sandratskii L M and Sasioglu E 2006 *Phys. Rev.* B **74** 214422
[36] Oguchi T, Terakura K and Williams A R 1983 *Phys. Rev.* B **28** 6443
[37] Liechtenstein A I, Katsnelson M I, Antropov V P and Gubanov V A 1987 *J. Magn. Magn. Mater.* **67** 65
[38] Cooke J F, Lynn J W and Davis H L 1980 *Phys. Rev.* B **21** 4118
[39] Savrasov S Y 1998 *Phys. Rev. Lett.* **81** 2570
[40] Karlsson K and Aryasetiawan F 2000 *Phys. Rev.* B **62** 3006
[41] Antropov V P 2003 *J. Magn. Magn. Mater.* **262** L192
[42] Katsnelson M I and Lichtenstein A I 2004 *J. Phys.: Condens. Matter* **16** 7439
[43] Anderson P W and Hasegawa H 1955 *Phys. Rev.* **100** 675
[44] van Schilfgaarde M and Mryasov O N 2001 *Phys. Rev.* B **63** 233205
[45] Kohgi Y, Ishikawa I and Endoh Y 1972 *Solid State Commun.* **11** 391
[46] Hutchings M T and Samuelsen E J 1972 *Phys. Rev.* B **6** 3447
[47] Goodenough J B and Kafalas J A 1967 *Phys. Rev.* **157** 389
[48] Roth W L 1958 *Phys. Rev.* **110** 1333
[49] Xu J L, van Schilfgaarde M and Samolyuk G D 2005 *Phys. Rev. Lett.* **94** 097201
[50] Gu R Y and Antropov V P 2005 *Preprint* cond-mat/0508781